Fluid Injection Influence on Fracture Propagation near an Underground Drift

Mohammad Youssef Fallah Soltanabad, Amade Pouya, Laurent Brochard, Lina-María Guayacán-Carrillo
Navier Laboratory/CERMES, Ecole des Ponts ParisTech, Gustave Eiffel University, CNRS, Marne la Vallée, France

Christophe De Lesquen, Minh Ngoc Vu
Andra R&D, Châtenay-Malabry, France

ABSTRACT: This study analyzes the propagation of fractures around a gallery submitted to fluid injection. After recalling some concepts of fracture modeling in a porous medium, 2D simulations are carried out with the finite element code Disroc®. These simulations account for the anisotropy of the in-situ stress state. The impact of hydro-mechanical couplings under the effect of fluid injection is addressed by three approaches of increasing complexity: 1- The pressure is assumed to act only in the existing fractures and in the tunnel with no coupling in the rock mass. 2- The pressure field is assumed stationary, obtained from an independent simulation, and used as an input for the mechanical calculation. 3- The transient flow of the fluid in the fracture and in the rock, mass is considered and coupled with the mechanics. A comparison of these approaches clarifies the various contributions of hydromechanical couplings on fracture propagation over different time horizons.

Keywords: Fracture propagation, porous media, underground storage, numerical modeling (FEM), hydromechanical coupling, Cohesive zone model (CZM).

1 INTRODUCTION

Generally, fluid fracturing is the process by which a fracture is generated and propagates as a result of fluid loading (i.e., pressure) applied by a fluid inside the fracture. Fluid fracturing modeling requires the coupling of at least three processes: (i) the mechanical deformation induced by the fluid pressure on the fracture surfaces; (ii) the flow of fluid within the fracture; and (iii) the fracture propagation. The rock's mechanical behavior is modeled as a linear poroelastic material. The criterion for fracture propagation is given by the well-known critical energy-release rate approach of linear elastic fracture mechanics (Griffith theory): the fracture propagates if the stress intensity factor at the tip exceeds the toughness of the rock.

There are many examples and applications of fluid fracturing in geomechanics. Magma-driven dykes are among natural examples, usually on the scale of tens of kilometers (Lister 1990, Rubin 1995, Spence et al.1985). Regarding applications, hydraulic fracturing of oil and gas reservoirs is a frequent reservoir stimulation technique (Mack et al. 2000). Fluid fracturing is also applied for the disposal of waste drill cuttings underground (Moschovidis et al. 2000), for the heat production from

geothermal reservoirs (Pine 1985), for fault reactivation (Board et al. 1992) in mining, and for the measurement of in situ stresses (Fairhurst 1964, Haimson 1993, Haimson & Cornet 2003).

In the framework of ANDRA's Cigéo project for the underground storage of radioactive waste in France, the fracture network generated around galleries dug in the Callovo-Oxfordian claystone is being studied. This fracturing exhibits a common mixed mode I / II propagation profile which results from the stress relaxation in the claystone due to excavation (Armand et al. 2014). In the long term, this fracture network is expected to undergo additional solicitation by gases (mainly H2) emitted by the long-term corrosion process of the metallic components of the repository and also arising from the radiolysis of the water. The accumulation of these gases could potentially affect the fracture network.

In this study, we investigate the role of hydro-mechanical couplings in the propagation of fractures around a gallery submitted to fluid injection, using FEM numerical modeling (Disroc® code). We address in particular the fluid flow and poro-mechanical couplings within both the rock (poroelasticity) and the fracture (cohesive zone model). In addition, we also assess the effect of the shear fracture geometry, and of the in-situ stress anisotropy.

2 METHOD

2.1 Poroelasticity

A porous medium is a solid that comprises a connected network of pores through which a fluid, liquid or gas, can circulate. The pore network and the solid part are described as a continuous biphasic medium which we refer to as the porous medium. We are interested in the mechanical and hydraulic behavior of this medium, which is the object of the well-accepted theory of poroelasticity (Coussy 2004, Cheng et al. 1993). In this study, the porous material is assumed to be fully saturated and under isothermal conditions, we consider Darcy's law for the fluid flow in the pore network, and Poiseuille law for the flow in the fracture.

2.2 Fracture mechanics

As for fracture propagation, its modeling is based on the concepts of energy release rate and stress intensity factors of fracture mechanics. These quantities fully characterize the severity of mechanical loading concerning fracture propagation, via the mechanical energy release upon propagation (energy release rate), or via the singularity of stresses and strains in the vicinity of the fracture front (stress intensity) (Anderson 2017). Although energy release and stress intensity may seem unrelated, it is not the case, and they are actually directly related (Bar1980; Anderson 2017). When loading is restricted to mode I, we have:

$$\frac{d}{da}(P-U) = G_I = \frac{K_I^2}{E_1} \quad (1)$$

where P is the work of the external forces applied to the fracture, U is the recoverable elastic deformation energy of the solid and a is the fracture length. The quantity $d/da\,(P-U)$ represents the dissipated energy per unit length of the fracture propagation, which defines the energy release rate G_I. K_I is the mode I stress intensity factor, and the above equation shows that it is fully determined by the energy release rate. According to the theory of fracture mechanics, fracture propagates when G_I reaches a critical value G_{Ic} (Anderson 2017). Conversely, fracture propagation occurs when the stress intensity also reaches a critical value K_{Ic} called toughness. G_{Ic} (or K_{Ic}) characterizes the resistance of the material to fracture propagation and are material properties, independent of the geometry or loading.

2.3 Numerical model

The numerical calculations are performed with the Disroc® code (Fracsima 2016). It is a Finite Element code enriched with joint elements, dedicated to the modeling of coupled thermo-hydro-mechanical phenomena in materials and structures in the presence of fracturing. In particular, it is

adapted to the consideration of discontinuities such as fractures, contact interfaces in materials, rock masses, and masonry structures, as well as linear inclusions such as bolts and tie rods in geotechnical structures and reinforcing fibers in composites.

2.4 Cohesive Zone Fracture with damage and plasticity

A way to numerically model the process of fracture propagation, consistent with the theory of fracture mechanics, is using the cohesive zone model. In particular, in this work, we consider the cohesive zone model for joint elements called ''CZFrac 21510'' (Fracsima 2016). This is an interface model that accounts for the damage process at the interface causing an irreversible degradation of the strength parameters (cohesion and tensile strength) and of the friction angle (Figure 1b). It describes the evolution of a rock joint-type interface, from a cohesive plane to a cohesionless frictional fracture. The model includes a softening behavior after peak stress (Figure 1 a).

(a) *(b)*

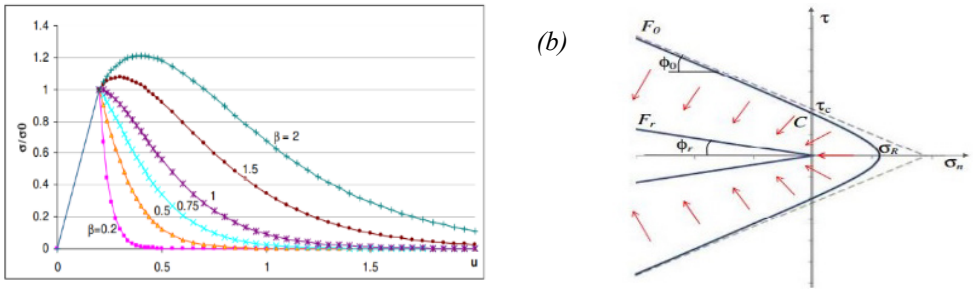

Figure 1. Cohesive zone fracture model (Fracsima 2016).

The cohesive law describing the stress-displacement relation at the interface is given by:

$$\tau = [(1-D)k_t + s\,k_{0t}]\,u_t^e \quad (2) \qquad \sigma_n = \left((1-\mathrm{D})k_n + \frac{S\,k_{0n}}{1+\frac{u_n}{e}}\right)u_n^e \quad (3)$$

where σ_n and τ are the normal and shear stresses, respectively, and u_n and u_t are the normal and tangent relative displacements across the interface, respectively. *D* is a damage variable varying from 0, for the initial intact state (rock joint), to 1 for the final entirely damaged state (fracture). The parameter k_{0t} represents the residual shear stiffness for the fully damaged interface, and k_{0n} represents the residual normal stiffness. Note that, in this equation, the compression stress σ_n is counted negatively and so is the displacement u_n corresponding to a closure. The parameter *e* represents the maximum closure, corresponding to an infinite compressive stress. Lastly, the parameter s ensures the unilateral contact condition for the fully damaged state: it takes only the values 0 (if $u_n > 0$) or 1 (otherwise).

On a series of benchmarks, the fracture propagation obtained with the CZFrac model proves to agree very well with the usual fracture mechanics (Fallah Soltanabad et al. 2023).

3 RESULTS

3.1 Geometries and parameters

The geometry of the model studied is a square of 200 m, representing the rock mass formation in which there is a tunnel at the center with a single shear-type fracture on the tunnel wall. The length of the initial fracture is 5.2 m, and the tunnel radius is 2.6 m. We studied two different directions of fracture: horizontal and vertical shear fractures, with two in-situ stress fields (isotropic at 12.55 MPa, and anisotropic at 12.55 MPa vertical and 16.1 MPa horizontal). An isotropic material is considered for the rock, with a Young's modulus of E= 5200 MPa and a Poisson's ratio of ν=0.3. The parameters

of the CZFrac model for the initial fracture are represented in Table 1. This initial fracture is fully damaged. The CZFrac model is also considered at all mesh interfaces in a domain around the crack (blue domain in Figure 2) but with no initial damage. The parameters for the undamaged zone are the same as the pre-existing fracture except for the following parameters: e=0.001 m, k_{0t}= 300 MPa/m, k_{0t}= 300 MPa/m, K_{IC}= 2.5 MPa.m$^{1/2}$. It should be noted that the toughness considered is larger than the actual toughness of the COx (0.25 MPa.m1/2), but this has a minor effect on the fracture propagation which is primarily controlled by the magnitude of the in-situ stress. A higher toughness makes it possible to consider coarser mesh by preventing spurious cracking far from the tip and thus avoiding numerical instabilities (Fallah Soltanabad et al. 2023).

Table 1. Mechanical parameters applied to the pre-existing fracture.

k_t	k_n	e	σ_R	C	φ	h_r	β	β'	k_{0t}	k_{0n}
3.00E+05 MPa/m	3.00E+05 MPa/m	0.00001 m	5.05 MPa	50 MPa	27°	1 -	0.1 -	1 -	30000 MPa/m	30000 MPa/m

3.2 *Effect of stress anisotropy*

We first consider a purely mechanical loading, with a uniform fluid pressure applied only inside the initial fractures and in the tunnel, and with no poromechanical coupling in the rock. Importantly, the pressure is not applied to the propagating fracture, which would lead to an unstable propagation. This simplistic loading can be viewed as the case of fluid pressurization on a short time scale with negligible transfer in the rock.

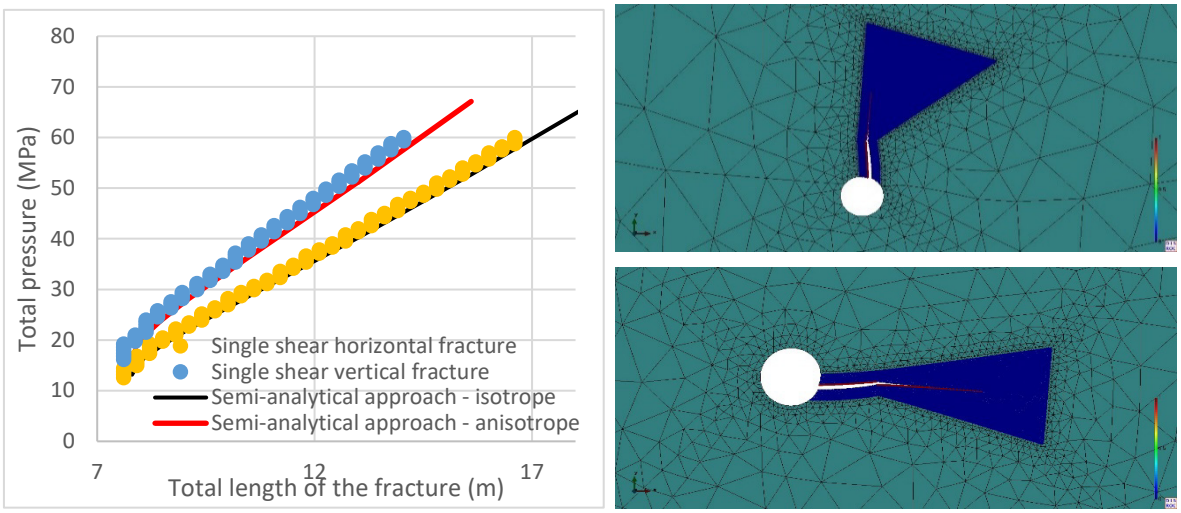

Figure 2. (left) Effect of stress anisotropy on the length of propagation for the single shear horizontal and vertical fractures and comparison with the semi-analytical approach. (right) geometry of the fracturing, for the cases of isotropic and anisotropic in-situ stresses (upper and lower part, respectively).

Figure 2 compares the cases of isotropic and anisotropic in-situ stresses. We display with yellow dots the fracture propagation for the isotropic case and with blue dots the anisotropic case. These results are quite consistent with theoretical estimates from fracture mechanics (black and red curves) based as above (Fallah Soltanabad et al. 2023), assuming straight horizontal and vertical fractures, which confirms the validity of the CZFrac modeling. It also shows that the curved shape of the shear fracture has little influence on the propagation, and the newly created crack mostly follows a radial path, irrespective of the initial fracture shape and in-situ stress. The length of propagation is smaller for the anisotropic stress case than for the isotropic case, which is the direct consequence of the higher stress orthogonal to the fracture (16.1 MPa instead of 12.55 MPa). Interestingly, in the anisotropic case, the fracture tends to propagate towards the radial direction, which suggests that the direction of

propagation is primarily controlled by the fluid pressurization, whereas the anisotropy of in-situ stress would tend to reorientate the propagation in the horizontal direction (direction of major stress).

3.3 Effect of fluid flow

In order to evaluate the effect of fluid flow (stationary or transient) on the poro-mechanical couplings, the fluid penetration in the porous medium is modeled with two scenarios: stationary flow (limit of a very long-time horizon) and transient flow (fluid pressure increase in 1s inside the tunnel, and then maintained constant for 1 day). In both cases, the hydro-mechanical couplings are accounted for both in the fracture and in the porous matrix. In this study, the hydromechanical coupling is made only from the hydraulic pressure field to the mechanics and therefore the mechanical calculation does not modify the hydraulic calculation. Moreover, the effect of fluid pressure is applied only to the pre-existing fracture, in order to compare with the purely mechanical fluid calculation of the previous section. We considered an initial Biot coefficient of 0.8 both in the rock and in the closed fracture. As the fracture opens, the Biot coefficient is changed to 1, so that the normal stress across the fracture is fully supported by the fluid. The permeability of the rock for the stationary and transient calculations is considered as an intermediary isotropic permeability which is: $k = 2.7\times10^{-20}\ m^{2.}$ Also, the storage coefficient for the rock is $C_M = 2.8\times10^{-4}\ (MPa)^{-1}$. For the flow in the pre-existing fracture, a hydraulic conductivity of $2.7\times10^{-17}\ m^3$ is considered. Finally, for the transient hydromechanics, the storage coefficient for the pre-existing fracture is: $C_{Mf} = e/K_f$ (K_f is the incompressibility modulus of the fluid).

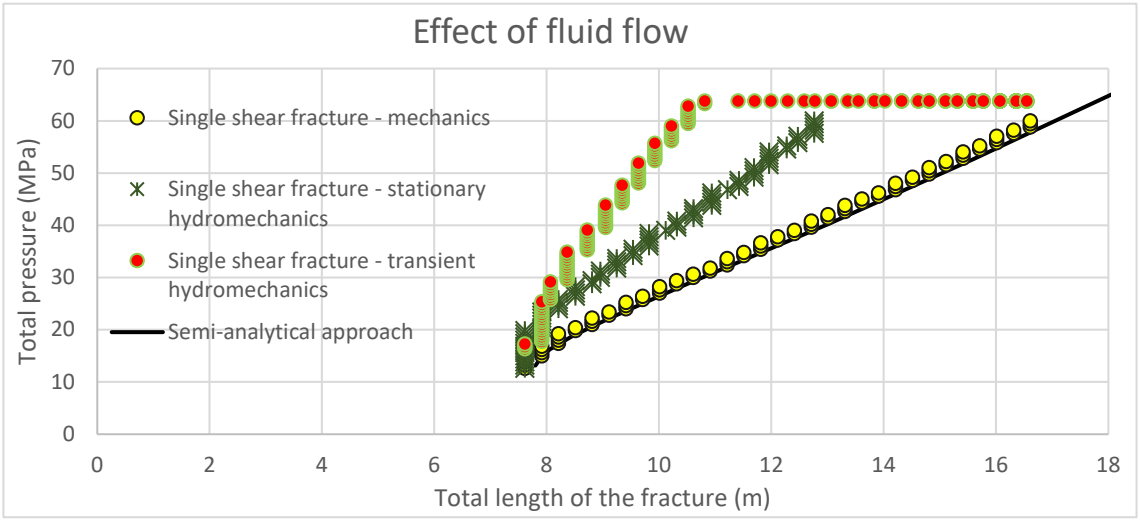

Figure 3. Effect of fluid flow on the propagation of fracture.

We display in Figure 3 the length of propagation as a function of the fluid pressure in the tunnel, for the three types of calculation (purely mechanical, stationary flow, and transient flow in an isotropic stress case). While, for the stationary calculation, the pressure field decreases smoothly from the tunnel to the boundary of the domain; for the transient calculation, the fluid has almost not diffused after the 1s of loading. Yet, after 1 day of maintaining the pressure, it fully filled the existing fracture but did not penetrate the rock, as a consequence of the large contrast between the permeability of the rock and that of the fracture. The stationary calculation exhibits significantly smaller propagations than the mechanical calculation because the pressure field inside the fracture is reduced, and because the poromechanical coupling in the rock opposes the propagation. The short time propagation of the transient case is even smaller, mainly because only the tunnel is loaded after 1s. But, as the fluid diffuses inside the fracture at constant tunnel pressure, it further propagates and after 1 day one recovers almost the same propagation as for the mechanical calculation. This is expected since the pressure field is then almost the same as for the mechanical calculation (full diffusion in the fracture but not in the rock).

4 CONCLUSIONS AND PROSPECTS

In this work, we performed numerical simulations of fracture propagation around a gallery submitted to fluid pressurization. Our case studies have shown that the in-situ stress anisotropy plays a significant role in the reactivation and propagation of fractures, in so far as propagation is mostly opposed by the stress orthogonal to the fracture. However, with this model, the fracture does not reorient in the most favorable direction with respect to the in-situ stress, but follows the radial path favored by the fluid loading. A significant effect of fluid pressure distribution in the rock matrix was observed on the length of propagation when the stationary pressure field was considered. The poromechanical coupling in the rock exposed to the stationary pressure field tends to act against fracture propagation. Finally, under transient conditions, before any significant fluid diffusion (1s) the propagation is even smaller than for the stationary case, but after 1 day (diffusion in the fracture but not in the rock) one recovers the simple mechanical case (constant pressure loading in the tunnel and fracture).

As perspectives for this study, various aspects that have been disregarded so far require a careful analysis: evolution of the flow and poromechanical coupling with fracture aperture, medium and fracture desaturation and gas dissolution in water, full coupling between fluid flow and mechanics, and long-term evolution with respect to nuclear waste applications.

REFERENCES

Anderson, T. L. 2017. *Fracture Mechanics: Fundamentals and Applications, Fourth Edition.* CRC Press.

Armand, G., Leveau, F., Nussbaum, C., La Vaissiere, R., Noiret, A., Jaeggi, D., Landrein, P., Righini, C. 2014. Geometry and Properties of the Excavation-Induced Fractures at the Meuse/Haute-Marne URL Drifts. *Rock Mech Rock Eng.*

Board, M., Rorke, T., Williams, G., Gay, N. 1992. Fluid injection for rock burst control in deep mining. In: Tillerson JR, Wawersik WR, editors. In: *Proceedings of the 33rd U.S. symposium on rock mechanics.* Rotterdam: Balkema; pp. 111–20.

Coussy, O. 2004. *Poromechanics*, John Wiley & Sons Ltd, pp. 113-145, 225-256.

Cheng, AHD., Abousleiman, Y., Roegiers, JC. 1993. Review of some poroelastic effects in rock. *International Journal of Rock Mechanics and Mining Sciences & Geomechanics Abstracts.* Vol. 30 (7), pp. 1119-1126.

Fairhurst, C. 1964. Measurement of in situ rock stresses, with particular reference to hydraulic fracturing. *Felsmech. Ingenieurgeol*. II 3-4, pp. 129-147.

Fallah Soltanabad, MY., Pouya, A., Brochard, L., Guayacán-Carrillo, LM., De Lesquen, C., Ngoc Vu, M. 2023. Fracture propagation around a gallery in claystone under fluid injection (soon to be published).

Fracsima. 2016. *Disroc, a Finite Element Code for modelling Thermo-Hydro-Mechanical processes in fractures porous media*, from http://www.fracsima.com/DISROC/Materials-Catalog.pdf.

Haimson, BC. 1993. The hydraulic fracturing method of stress measurement: theory and practice. In: *Hudson J, editor. Comprehensive rock engineering,* Vol. 3. Oxford: Pergamon Press; p. 395–412.

Haimson, BC., Cornet, F.H. 2003. ISRM Suggested Methods for rock stress estimation—Part 3: hydraulic fracturing (HF) and/or hydraulic testing of pre-existing fractures (HTPF), *International Journal of Rock Mechanics and Mining Sciences*, Vol. 40 (7–8), pp. 1011-1020, ISSN 1365-1609.

Lister, JR. 1990. Buoyancy-driven fluid fracture: the effects of material toughness and of low-viscosity precursors. *Journal of Fluid Mechanics*, Vol. 210, pp. 263–280.

Mack, MG., Warpinski, NR. 2000. Mechanics of hydraulic fracturing. In: *Economides, Nolte, editors. Reservoir stimulation.* 3rd ed. Chichester, Wiley: [Chapter 6].

Moschovidis, Z., et al. 2000. The Mounds drill-cuttings injection experiment: final results and conclusions. In: *Proceedings of the IADC/SPE drilling conference,* New Orleans, pp. 23–25. Richardson: Society of Petroleum Engineers, [SPE 59115].

Pine, RJ., Cundall, PA. 1985. Applications of the Fluid-Rock Interaction Program (FRIP) to the modelling of hot dry rock geothermal energy systems. In: *Proceedings of the international symposium on fundamentals of rock joints,* Bjorkliden, Sweden, pp. 293–302.

Rubin, AM. 1995. Propagation of magma-filled cracks. *Ann Rev Earth Planet Sci*, Vol. 23, pp. 287–336.

Spence, DA., Turcotte, DL. 1985. Magma-driven propagation crack. *J Geophys Res*, Vol. 90, pp. 575–580.